Annu. Rev. Mater. Res. 2006. 36:199–230
doi: 10.1146/annurev.matsci.36.022805.094757

First published online as a Review in Advance on March 7, 2006

PROGRESS IN PLASTIC ELECTRONICS DEVICES

Th. Birendra Singh and Niyazi Serdar Sariciftci
Linz Institute of Organic Solar Cells (LIOS), Physical Chemistry, Johannes Kepler University of Linz, A 4040, Linz, Austria; email: Birendra.Singh@jku.at, Serdar.Sariciftci@jku.at

Key Words organic field-effect transistors, organic semiconductor, morphology, interfacial layer

■ **Abstract** Organic field-effect transistors (OFETs) based on solution-processible polymeric as well as small molecular semiconductors have shown impressive improvements in their performance during recent years. These devices have been developed to realize low-cost, large-area electronic products. This review gives an overview of the materials' aspect, charge-transport, and device physics of OFETs, focusing mainly on the organic semiconductor and organic dielectric materials and their mutual interface. Recent developments in the understanding of the relationship between microstructure and charge transport, the influence of processing techniques, and gate dielectric are reviewed. Comparative data of charge-carrier mobility of most organic semiconductors have been compiled. Ambipolar charge transport in OFETs and its applications to integrated circuits as well as ambipolar light-emitting transistors are also reviewed. Many interesting questions regarding how the molecular and electronic structures at the interface of the organic semiconductor and organic insulator influence device performance and stability remain to be explored.

INTRODUCTION

Organic thin-film electronics has developed, with intense effort in numerous academic and industrial research laboratories, into a promising technology in the past two decades, with demonstrated prototypes of organic integrated circuits for radio frequency identification tags (1, 2) and thin-film transistor (TFT) arrays for active matrix displays (3). Organic field-effect transistors (OFETs) have also been fabricated in arrays to drive electrophoretic display pixels (4). To date Bell Labs, using vacuum evaporation techniques, has succeeded in making organic integrated circuits with as many as 1888 transistors (2). Using the same techniques, Infinion Technology achieved similar results with the realization of integrated circuits on special papers (5). Polymer Vision, Philips Research Laboratory came up with a flexible 4.7-inch QVGA active matrix display containing 76,800 organic transistors (6). As the number of transistors per circuit increases, there is an increasing need for circuits characterized by low power dissipation, high noise margin, and greater operation stability. The performance of the individual

transistor limits the switching speed in an integrated circuit, which can be roughly estimated by the ratio of mobility to channel length of the transistor (3). To obtain higher switching speed, the search for higher mobility materials is therefore important along with the effort to downscale the transistor geometry. Current benchmarks for high mobility materials among various organic semiconductors are pentacene (7) and fullerenes (for both $\mu \sim 6\ cm^2\ Vs^{-1}$) (8, 9) for *p*-type and *n*-type, respectively.

This chapter gives an overview of organic semiconductors as well as organic gate insulators used in OFETs in terms of their processing and interfacial characteristics. The device physics of OFETs is also described qualitatively for an understanding of the charge transport and charge trapping at the active semiconductor/dielectric interface. Owing to space limitations, no attempt is made to review the physics of gate dielectrics nor to give an overview of single-crystal OFETs. For these important subjects we refer the reader to other excellent and recent review articles (1, 10, 11).

Device Geometry

OFETs have been fabricated with various device geometries, as depicted in Figure 1*a–d*. The most commonly used device geometry is a bottom gate with top contact, partly because it borrows the concept of silicon TFT, using thermally grown Si/SiO_2 oxide as gate dielectric. Because it is a commercially available high-quality Si/SiO_2 substrate, this device geometry has dominated the field. Recently it was shown that organic dielectrics are also promising for high-performance OFETs (8, 9, 12–22). Organic dielectrics (*i*) can be solution-processed, (*ii*) provide smooth films on transparent glass and plastic substrates, (*iii*) are suitable for optoelectronics like photoresponsive OFETs owing to their high optical transparency, (*iv*) can be thermally stable up to 200°C with a relatively small thermal-expansion coefficient, and (*v*) can possess a rather high dielectric constant up to 18.

The immediate opportunity of use of organic dielectric is also for the top-gate-structured OFET, as depicted in Figure 1*c*,*d*, as an organic dielectric does not destroy the underlying organic semiconductors. Top-gate/bottom-contact-structured devices allow patterning of the bottom source-drain electrodes on top of any flexible or rigid substrate prior to fabricating the rest of the device. Top-gate/top-contact-devices allow organic semiconductor films to grow on top of any flexible or rigid substrate. Figure 1 illustrates the most widely used configurations of OFET elements; nevertheless, there exist several alternative ways of arranging the device elements.

Operating Principle of OFETs

A poly(2,5-thienylene vinylene) (PTV) OFET (Figure 2*a*) is used here to describe typical OFET device characteristics and the methods used to calculate the mobility μ and the I_{on}/I_{off} ratio (which is the ratio of the current in the accumulation mode

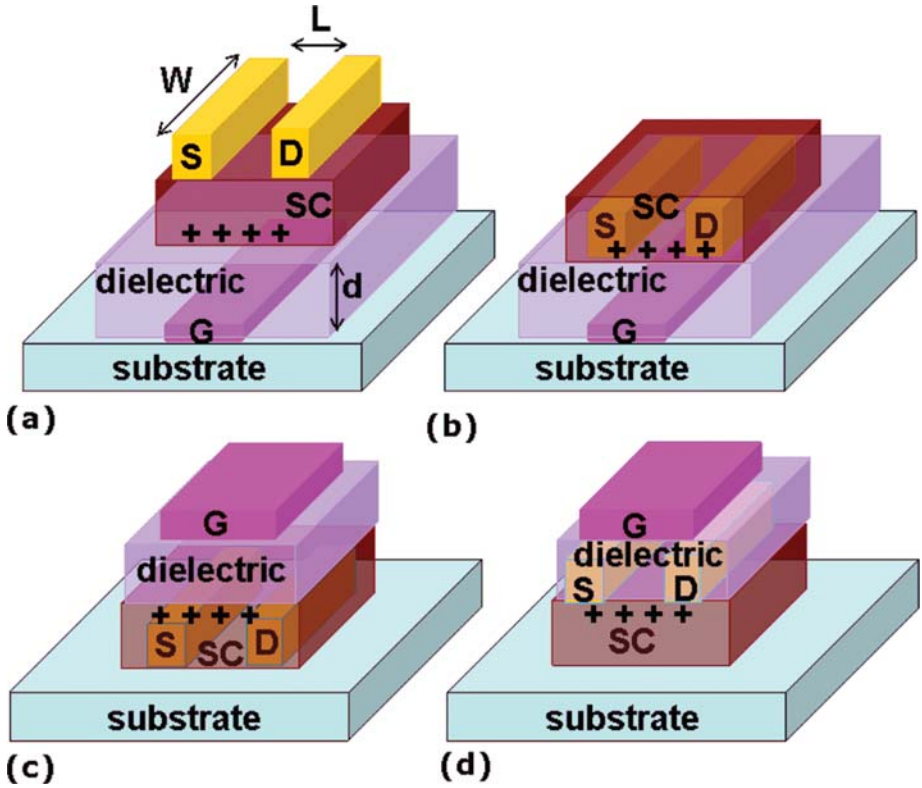

Figure 1 Schematic of bottom-gate organic field-effect transistors (OFETs) with (*a*) top-contact (staggered) or (*b*) bottom-contact (coplanar) structures. Schematic diagram of (*c*) top-gate/bottom-contact OFETs using standard TFT device structures and (*d*) top-gate/top-contact OFETs is also shown.

over the current in the depletion mode). The OFET *I–V* characteristics can be adequately described by standard models (23–26). Figure 2*b* shows a typical plot of drain-source current I_{ds} versus drain-source voltage V_{ds} at various gate voltages V_g, which corresponds to a device using PTV as the semiconductor, 500-nm spin-coated polymethyl-methacrylate (PMMA) as the gate insulator on top of heavily doped Si substrate as gate electrode, and gold source and drain electrodes in top-contact geometry, as depicted in Figure 2*a*.

At low V_{ds}, I_{ds} increases linearly with V_{ds} (linear regime) and is approximately determined from the following equation:

$$I_{ds} = \frac{WC_i}{L}\mu(V_g - V_T)V_{ds} \qquad 1.$$

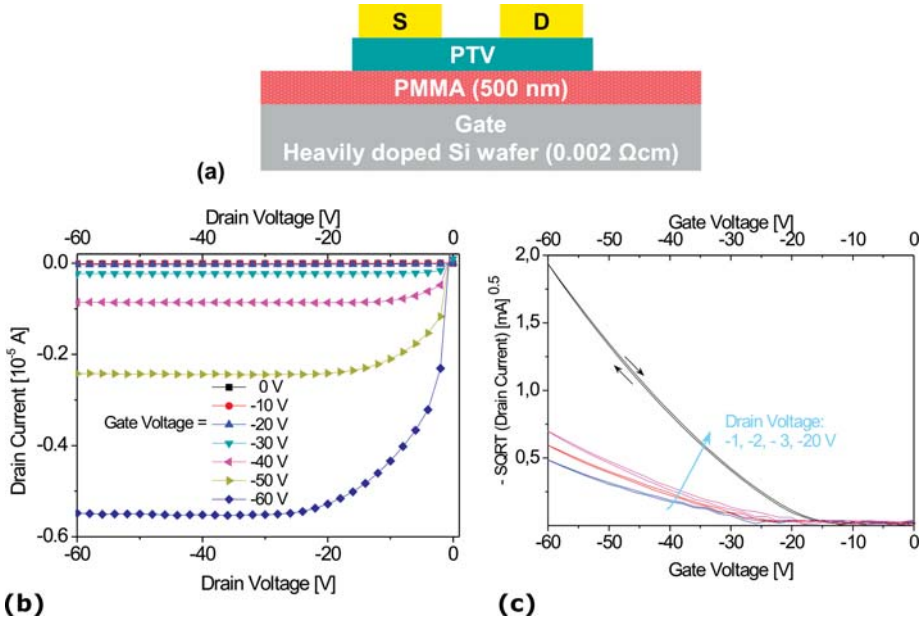

Figure 2 (*a*) Scheme of a top-contact PTV OFET. (*b*) Output characteristics (drain-source current, I_{ds}, versus drain-source voltage, V_{ds}) of a *p*-channel PTV OFET fabricated and measured in the authors' laboratory. (*c*) Transfer characteristics ($\sqrt{I_{ds}}$ versus gate voltage, V_g, for different V_{ds}) with arrows indicating the forward and reverse directions of sweeping of V_g. Linear field-effect mobility of 7×10^{-4} cm^2 Vs^{-1} and saturated mobility of 1×10^{-3} cm^2 Vs^{-1} can be extracted from these devices with channel length L of 25 μm and channel width W of 1.4 mm ($W/L = 40$).

where L is the channel length, W is the channel width, C_i is the capacitance per unit area of the insulating layer, V_T is the threshold voltage, and μ is the field-effect mobility. The latter can be calculated in the linear regime from the transconductance, g_m,

$$|g_m|_{linear} = \left(\frac{\delta I_{ds}}{\delta V_g}\right)_{V_{ds}=constant} = \frac{W}{L}\int_0^{V_{ds}} \mu C_i dV = \frac{WC_i}{L}\mu V_{ds} \qquad 2.$$

by plotting I_{ds} versus V_g at low V_{ds} and equating the value of the slope of this plot to g_m.

Figure 2*c*, which corresponds to Figure 2*b*, shows such a plot, and the calculated mobility value is 7×10^{-4} cm^2 Vs^{-1} at $V_{ds} = -2$ V. The value of V_{ds} is chosen so that it lies in the linear part of the I_{ds}-versus-V_{ds} curve. For this device, L was equal to 25 μm, and W was equal to 1.4 mm. The current modulation (I_{on}/I_{off}) for the device of Figure 2*a* is slightly above 10^3 when V_g is scanned from 0 to −60 V (Figure 2*c*). When V_{ds} is more negative than V_g, I_{ds} tends to saturate (saturation

regime) owing to the pinch-off of the accumulation layer, and this regime is modeled by the following equation:

$$I_{ds} = \frac{\mu W C_i}{2L}(V_g - V_T)^2 \qquad 3.$$

In the saturation regime, μ can be calculated from the slope of the plot of $\sqrt{I_{ds}}$ versus V_g, as shown in Figure 2*c*. For the same device as in Figure 2*a*, the mobility calculated in the saturation regime was 1×10^{-3} cm^2 Vs^{-1}. The difference between calculated mobility values is assigned to higher charge-carrier density in the saturation regime as compared with that of the linear regime.

To demonstrate the operating principle of the OFETs, a simplified energy-level diagram for Fermi level of source-drain metal electrode and HOMO-LUMO levels of a semiconductor are shown in Figure 3. If there is no gate voltage applied (Figure 3*a*), the organic semiconductor, which is intrinsically undoped, will not show any charge carriers. Direct injection from the source/drain electrodes is the only way to create flowing current in the organic semiconductor. Such currents will be relatively small owing to the high resistance of the organic semiconductors and large distance between the source and drain electrodes.

When a negative gate voltage is applied (Figure 3*b*), positive charges are induced at the organic semiconductors adjacent to the gate dielectric (a *p*-type conducting channel is formed). If the Fermi level of the source/drain metal is close to the HOMO level of the organic semiconductor, then positive charges can be extracted by the electrodes by applying a voltage, V_{ds}, between the drain and source. Such organic semiconductors with the ability to conduct only positive-charge carriers are termed *p*-type semiconductors.

When a positive voltage is applied to the gate (Figure 3*c*), negative charges are induced at the semiconductor adjacent to the dielectric interface (an *n*-type conducting channel is formed). If the Fermi level of source/drain metal is far away from the LUMO level such that electron injection/extraction is very unlikely, then low I_{ds} is expected owing to high contact barriers. If the Fermi level of source/drain metal is close to the LUMO level of the organic semiconductor, then negative charges can be injected and extracted by the electrodes by applying a voltage, V_{ds}, between the drain and source. Such organic semiconductors with ability to conduct only negative-charge carriers are said to be *n*-type semiconductors. In some organic semiconductors, both electrons and holes can be injected and transported, an effect known as ambipolar transistor that is discussed below.

Recently, significant improvements in charge-carrier mobilities of organic semiconductor materials in OFETs have been made (see Table 1). However, in these devices, choice of gate dielectrics play a crucial role. Whereas most of the organic semiconductor materials are *p*-type semiconductors and sustain positive-charge-carrier conduction, *n*-type organic semiconductors are less represented, mostly because of the difficulty of synthesizing materials with a large electron affinity that allows the injection of electrons from stable electrodes in air. It is also generally appreciated to have a balanced electron and hole mobility in an ambipolar

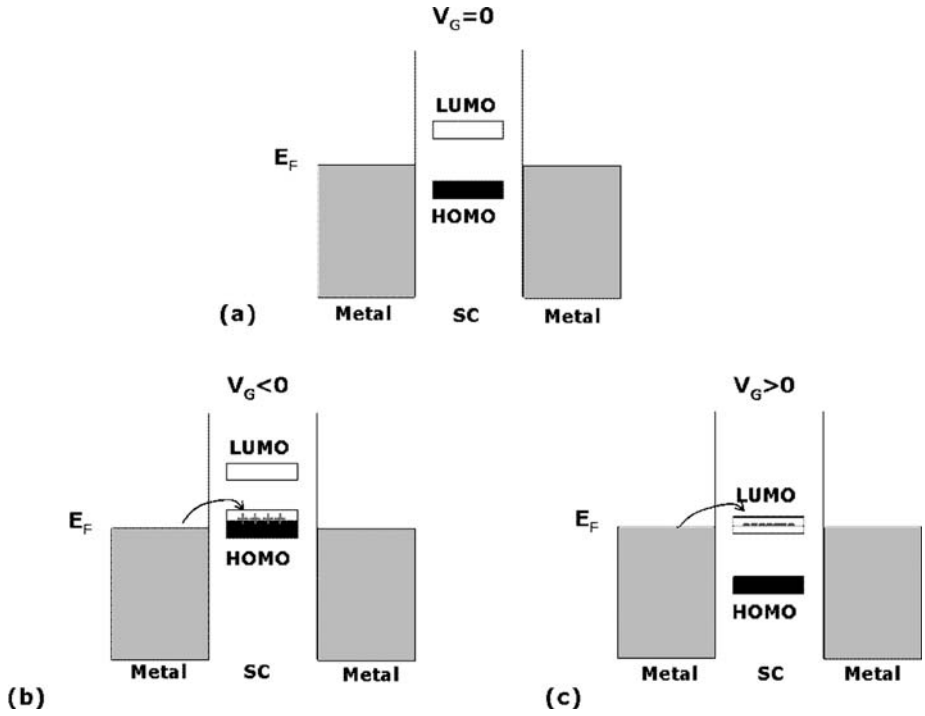

Figure 3 Illustration of an OFET working principle with respect to applied V_g. (*a*) No charges are injected when $V_g = 0$ V. (*b*) When a negative voltage is applied to the gate, positive charges are induced at the organic semiconductor/organic insulator interface (at the channel). When the Fermi level of source/drain metal is close to the HOMO level, holes can be injected from/to the metal to/from the HOMO of the semiconductor, and a *p*-type OFET is realized. (*c*) When a positive voltage is applied to the gate, negative charges are induced at the organic semiconductor/organic insulator interface and for source/drain metals with Fermi levels close to the LUMO level of the organic semiconductor, electrons can be injected from the source/drain metal to the LUMO of the semiconductor, and an *n*-type OFET is realized.

material for use in organic complementary metal oxide semiconductor (CMOS)–like circuits and in possible applications for organic light-emitting transistors (OLETs).

OFET MATERIALS

Solution-processible materials are very attractive for use in organic electronics, in part because films exhibiting good characteristics can often be formed simply by spin coating, casting, or printing at low temperatures and under ambient conditions. From this point of view, soluble and processible polymeric semiconductors offer

TABLE 1 Highest field-effect mobility (μ) values measured from OTFTs as reported in the literature annually from 1986 through 2005.

Year	Mobility ($cm^2\ Vs^{-1}$)	Material (deposition method)[a]	I_{on}/I_{off}[b]	W/L	Reference
1983	Minimal, not reported (NR)	Polyacetylene (s) (demonstration of field effect in an OTFT)	NR	200	[108]
1986	10^{-5}	Polythiophene (s)	10^3	NR	[109]
1988	10^{-4}	Polyacetylene (s)	10^5	750	[110]
	10^{-3}	Phthalocyanine (Pc) (v)	NR	3	[111]
	10^{-4}	Poly(3-hexylthiophene) (s)	NR	NR	[112]
1989	10^{-3}	Poly(3-alkylthiophene) (s)	NR	NR	[113]
	10^{-3}	α–ω-hexathiophene (v)	NR	NR	[46]
1992	0.027	α–ω-hexathiophene (v)	NR	100	[114]
	2×10^{-3}	Pentacene (v)	NR	NR	[114]
1993	0.05	α–ω-di-hexyl-hexathiophene (v)	NR	100 –200	[45]
1994	0.06	α–ω-dihexyl-hexathiophene (v)	NR	50	[47]
1995	0.03	α–ω-hexathiophene (v)	$>10^6$	21	[51]
	0.038	Pentacene (v)	140	1000	[115]
	0.3	C_{60} (v)	NR	25	[85]
1996	0.02	Pc (v)	2×10^5	NR	[58]
	0.045	Poly(3-hexylthiophene) (s)	340	20.8	[92]
	0.13	α–ω-dihexyl-hexathiophene (v)	$>10^4$	7.3	[53]
	0.62	Pentacene (v)	10^3	11	[116]
1997	1.5	Pentacene (v)	10^8	2.5	[82]
	0.05	Bis(dithienothiophene) (v)	10^8	500	[117]
1998	0.1	Poly(3-hexylthiophene) (s)	$>10^6$	20	[91]
	0.23	α–ω-dihexyl-quaterthiophene (v)	NR	1.5	[118]
	0.15	Dihexyl-anthradithiophene	NR	1.5	[119]
2000	0.1	*n*-decapentafluoroheptyl-methylnaphthalene-1,4,5,8-tetracarboxylic diimide (v)	10^5	1.5	[120]
	0.1	α–ω-dihexyl-quinquethiophene (s)	NR	NR	[120]
2002	3	Pentacene (v)	10^5	1.3	[121]
	0.6	*N,N′*-dioctyl-3,4,9,10-perylene tetracarbozylic diimide (v)	10^5	10	[122]
2003	0.001	CuPc (v)	2.3×10^4	165	[63]
	0.002	Methanofullerene [6,6]-phenyl-C61-butyric acid methyl ester (PCBM) (s)	NR	140	[66]
	0.53	C_{60} (v)	10^8	40	[87]
	3.3	Pentacene (v)	1.6×10^6	10	[81]
	6	Pentacene (v)	do	do	[7]
	0.18	3′,4′-dibutyl-5–5bis(dicyanomethylene)-5,5′-dihydro-2,2′:5′,2′′-terthiophene (DCMT)	10^6	10	[123]

(*Continued*)

TABLE 1 (*Continued*)

Year	Mobility ($cm^2\ Vs^{-1}$)	Material (deposition method)[a]	I_{on}/I_{off}[b]	W/L	Reference
2004	0.73	Poly(3-hexylthiophene) (s)	NR	12	[124]
	0.1	PTCDI-C_5 (v)	10^5	10	[125]
	0.004	C_{60} (v)	10^5	250	[126]
	0.2	PCBM (s)	10^3	23	[21]
	0.1	P3HT (s)	10^5	200	[127]
	0.01	PCBM (s)	10^6	25	[67]
2005	0.63	C_{60} (v)	10^4	40	[88]
	0.015	Poly(3,3′′-dialkyl-terthiophene)(s)	10^5	50	[128]
	6	C_{60} (v)	10^4	40	[8]
	0.51	Pentacene (v)	10^5	40	[129]
	0.06	C_{60}-fused *N*-methylpyrrolidine-*meta*-C12 phenyl (C60MC12) (s)	1.6×10^5	250	[68]
	0.02	PCBM (s)	7×10^4	250	[68]
	0.15	Thieno[2,3-b]thiophene(s)	10^5	NR	[33]

[a]v, vacuum deposition; s, from solution.

[b]Values for I_{on}/I_{off} correspond to different gate voltage ranges and thus are not readily comparable to one another. The reader is encouraged to read the details of the experiments in the cited references.

greater potential than do vacuum-evaporated small molecular organic semiconductors. Currently, semiconducting polymers with considerable air stability and high charge-carrier mobility are a subject of intense research interest for OLEDs and organic solar cells as well as organic transistors. To achieve high performance, solution-processible organic semiconductors with high charge mobilities ordered structures are needed at the tertiary nanostructure of organic thin films. One route involves (*a*) designing the material to exhibit microcrystallinity (27) or liquid crystallinity (28) or self-organization or (*b*) making use of specific interactions with a templating substrate. The other approach aims to produce a completely amorphous micro/nanostructure to provide a uniform path for charge transport, with a minimum degree of site-energy fluctuations (29). Amorphous micro/nanostructures may be more advantageous than the partially crystalline nanomorphologies because the crystalline domains with lower energies embedded in an amorphous matrix of the same material act as trap sites; the crystalline packing lowers the energy locally in such domains.

P3HT is microcrystalline in thin-film form and has one of the high charge-carrier mobilities. Its ionizaion potential (typically approximately 4.9–5.0 eV) is best suited to form ohmic contact with many air stable electrodes such as Au or the conducting polymer polyethylenedioxy-thiopehene doped with polystyrene sulfonic acid (PEDOT/PSS). However, P3HT tends to exhibit a large positive threshold voltage, V_T, shift upon exposure to air, presumably owing to doping of the polymer (30). P3HT is known to form a charge-transfer complex with oxygen (31). This can be improved by increasing the ionization potential of the polythiophene backbone by either adopting a fully planar conformation through

the side-chain substitution pattern (32) or by incorporating partially conjugated comonomers into the main chain (33). Field-effect mobilities exceeding 0.15 cm^2 Vs^{-1} have been reported from such materials in air (Figure 4).

Increasing the performance of the semiconducting polymers through doping results in a high source/drain current at zero gate voltage. Polyfluorene (34, 35), P3HT, and most solution-processed polymers generally show *p*-type semiconducting nature. Recently, the University of Cambridge group has shown ambipolar

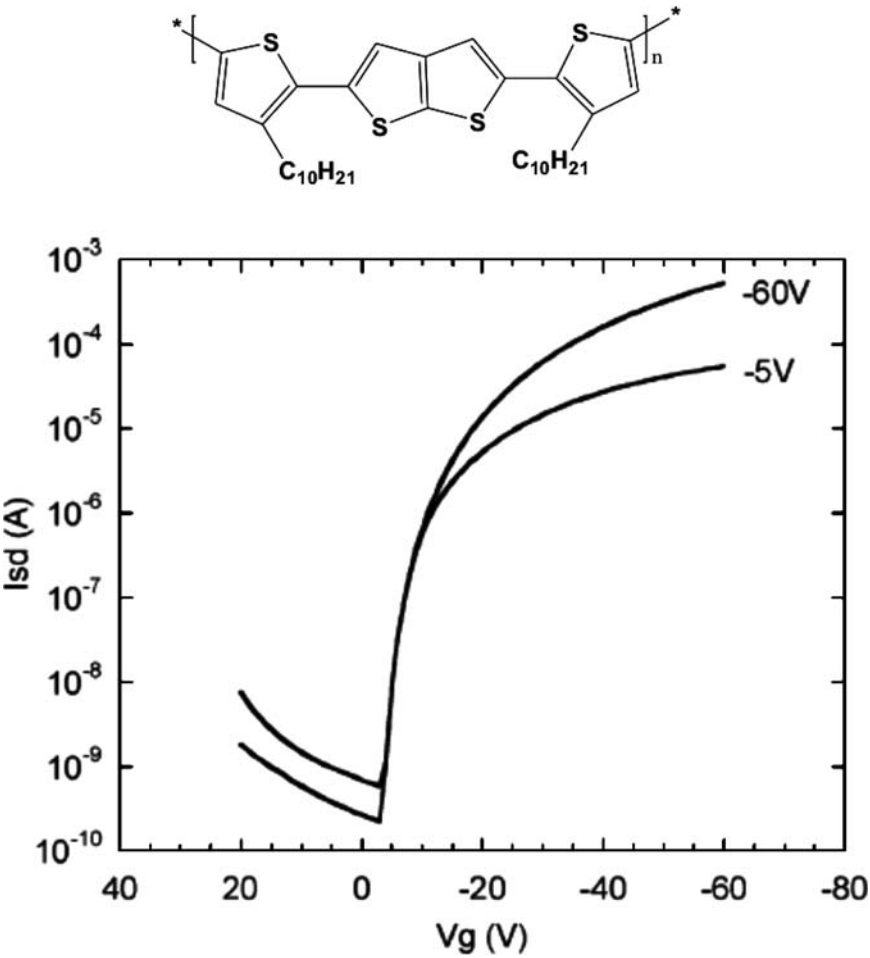

Figure 4 (*Top*) Chemical structure of a polythiophene-based semiconductor incorporating thieno[2,3-b]thiophene. (*Bottom*) Transfer characteristics of an OFET realized using the polymer (*top*) as a semiconductor in air scanned from positive to negative gate voltages at drain voltages of −5 V and −60 V. Reproduced with permission from Reference 33.

transport in OFETS for solution-processed semiconducting polymers (22) by avoiding the charge-carrier trapping at the interface of the insulator.

An alternative route to making solution-processible polymeric materials is to use small-molecule semiconductors processed either from the solution or evaporated (sublimated) from a heated source onto a target substrate. Such an example is pentacene, an aromatic compound with five condensed benzene rings. Pentacene has been widely studied as a *p*-type semiconductor for OFETs. The highest field-effect mobility obtained is 3 $cm^2\ Vs^{-1}$ for pentacene thin film on polymer dielectric (13) and 6 $cm^2\ Vs^{-1}$ on a chemically modified SiO_2/Si substrate (7). Among the *n*-type semiconductors, fullerene and its derivatives have been widely studied; these reach a field-effect mobility of 6 $cm^2\ Vs^{-1}$ with hot wall epitaxy–grown fullerene thin films on polymeric dielectrics (8, 9). Small-molecule organic semiconductors can also be rendered solution processible by attachment of flexible side chains. Among the fullerene derivatives, phenyl C_{61}-butyric acid methyl ester (PCBM) has a mobility as high as 0.2 $cm^2\ Vs^{-1}$ when the film is solution cast on polymeric dielectrics (21). Some of the side chain–substituted small molecules that exhibit liquid-crystalline phases at elevated temperatures provide alternative routes to forming highly crystalline thin films from solution. Discotic liquid-crystalline molecules, such as hexabenzocoronenes, uniaxially aligned in thin-film form with the columnar axis oriented along the transport direction in the OFETs, have field-effect mobilities up to 0.01 $cm^2\ Vs^{-1}$ along the discotic columns. Use of graphoepitaxy on highly crystalline teflon alignment layers (36) or deposition by zone crystallization (37) results in such an orientation. Polycrystalline thin films of a conjugated molecule can be obtained by forming a thin film of a soluble precursor on the substrate with subsequent thermal (38) or irradiative (39) conversion into the fully conjugated form. Pentacene precursors have been reported to yield field-effect mobilities of 0.01–0.1 $cm^2\ Vs^{-1}$ (40) or 0.1–0.8 $cm^2\ Vs^{-1}$ (41) after thermal conversion at 150–200°C. A precursor-route approach to tetrabenzoporphyrin has also been developed (42); this yields a field-effect mobility on SiO_2 of 0.02 $cm^2\ Vs^{-1}$ after thermal conversion at 150–200°C. Sexithiophene substituted with ester groups, which can be removed by thermolysis at 150–260°C, exhibits field-effect mobilities on SiO_2 of up to 0.07 $cm^2\ Vs^{-1}$ (43).

Conjugated oligothiophene's charge-carrier mobility can be improved by adding alkyl chains to the end of the oligothiophene rings (44). Among all the thiophene oligomers, α-sexithiophene (α-6T) and its derivatives have been widely used as active organic materials (45–48). Carrier mobilities reported for α-6T OFETs have improved from 10^{-4} $cm^2\ Vs^{-1}$ to greater than 0.01 $cm^2\ Vs^{-1}$ (49–54). Halik and coworkers (55) recently reported obtaining a carrier mobility of 1.1 $cm^2\ Vs^{-1}$ for alkyl-substituted oligothiophene. They synthesized and evaluated a series of alkyl-substituted oligothiophenes with different alkyl side-chain lengths and different chromophore lengths ranging from four to six thiophene units. They found that the OFETs' performance depends critically on the length of the side chains. The highest mobility was found for α,α'-diethylsexithiophene, which, owing to its shorter side chains, forms a significantly thinner barrier between the conjugated

backbones, leading to more efficient carrier tunneling. Para-sexiphenyl (PHP), a large band-gap oligomer, has mobilities in the range of 10^{-2} cm^2 Vs^{-1} (56, 57).

Phthalocyanines (Pcs) as organic semiconductors have been studied widely owing to their intense optical absorptions and excellent optoelectronic properties (58, 59). They have been used in solar cells, optical limiters, and photoconductors (60, 61). Mobilities up to 0.11 cm^2 Vs^{-1} for OFETs are reported for metallophthalocyanines (62). Bao and coworkers (63) observed ambipolar transport in Pc-based OFETs. Substituted Pcs have electronic levels that can be shifted in a wide range by appropriate substitution with electron-withdrawing ligands, with heteroatoms, or with electron-withdrawing substituents like chlorine or fluorine atoms to their outer rings (64, 65).

Soluble forms of fullerenes such as methanofullerene and PCBM have high mobility (10^{-3} to 0.2 cm^2 Vs^{-1}) (21, 66, 67) and show generally *n*-type semiconductor properties. Recently it has been shown that PCBM also has ambipolar transport (67). Regarding the transport properties of soluble fullerenes, recent reports of long-chain alkyl-substituted C_{60}, C_{60}-fused *N*-methylpyrrolidine-meta-C12 phenyl (C60MC12), show a less temperature-dependent mobility, with activation energy ∼20 meV, as shown in Figure 5. PCBM shows much higher activation energy, of the order of 60–100 meV (21, 68).

The several organic dielectrics used in OFETs clearly show the variability and the versatility of using organic gate insulators. The physics of organic dielectrics is a well-developed branch of science and technology and is not further discussed here. We simply display the chemical structures of commonly used organic dielectrics (Figure 6), along with organic semiconductors with *p*-type (Figure 7) and *n*-type (Figure 8) in OFETs. The insulator also plays a crucial role; insulating materials and deposition techniques used for these materials are reviewed elsewhere (10).

CRITICAL PARAMETERS INFLUENCING OFET FABRICATION AND PERFORMANCE

In the early days of organic TFTs, it appeared more convenient to use well-known techniques such as thermal oxidation or photolithography, and most of the devices were actually produced on oxidized silicon with source and drain contacts patterned with conventional lithography. However, to adapt to the demand for low-cost and easy-fabrication techniques, there is a trend of patterning the source-drain electrodes first, as shown for the top-gate geometry devices in Figure 1 *c*, *d*. An elegant and promising route to low-cost fabrication of organic integrated circuits is the direct printing of various elements that constitute OFETs. These include

1. screen printing (69),
2. roll-to-roll printing (70),

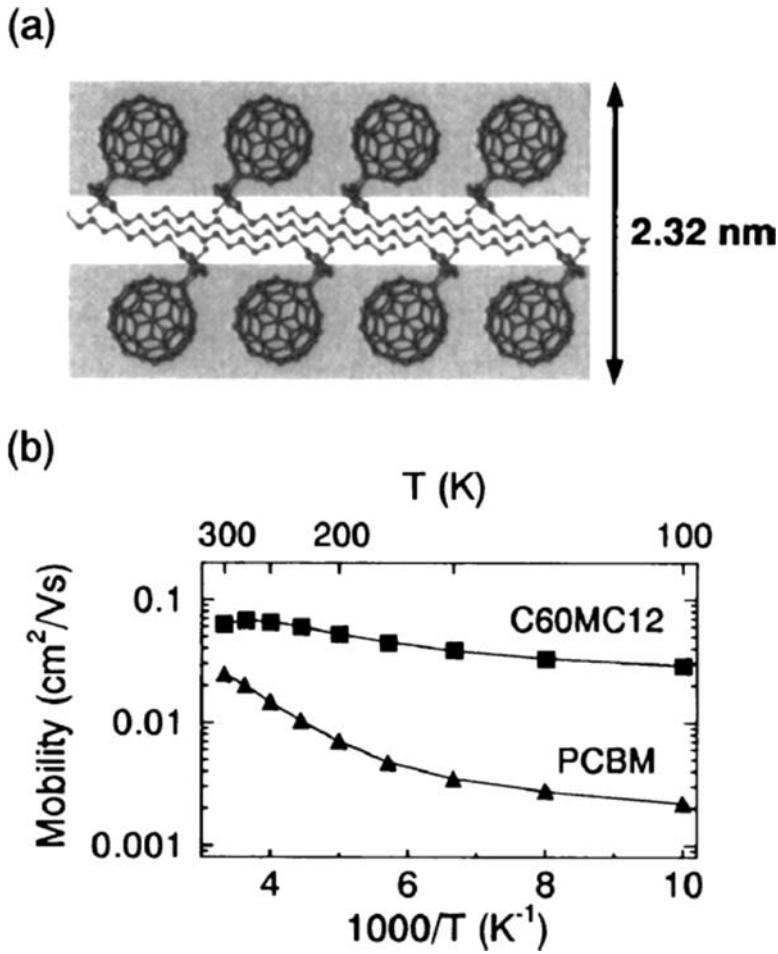

Figure 5 (*a*) Illustration of schematic film structure of C60MC12 active layer. (*b*) Temperature dependence of the field-effect mobility extracted from the characteristics of C60MC12- and PCBM-based OFETs in the saturation regime $V_{ds} = 50$ V. Reproduced with permission from Reference 68.

3. microcontact printing (71),
4. inkjet printing (72–75),
5. thermal imaging (76), and
6. offset printing (5, 77).

These printing methods can provide a resolution down to 2 μm.

Another popular technology is vacuum evaporation using shadow masks. Hot wall epitaxy (HWE) is a special growth method (78) that works close to

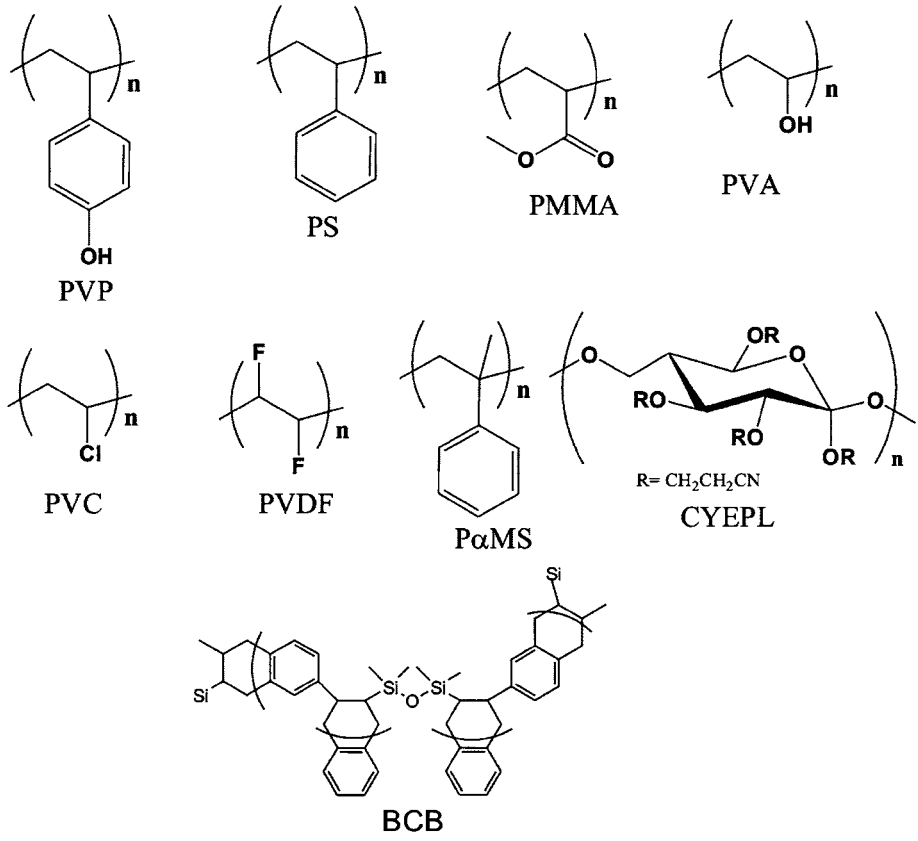

Figure 6 Chemical structures of some commonly used organic dielectrics. PVP, poly(4-vinyl phenol); PS, polystyrene; PMMA, polymethyl-methacrylate; PVA, polyvinyl alcohol; PVC, polyvinylchloride; PVDF, polyvinylidenfluoride; PαMS, poly[α-methylstyrene]; CYEPL, cyano-ethylpullulan; BCB, divinyltetramethyldisiloxane-bis(benzocyclobutene).

thermodynamic equilibrium and that results in well-ordered organic thin films with high OFET mobilities (8, 9).

For all fabrication methods used, the morphology of organic semiconductors as well as that of the organic dielectric interface has been found to have critical importance.

The Interfacial Layer between the Organic Semiconductor and the Dielectric

α-6T OFETs (46, 79) are used to demonstrate that the accumulation layer resides within one layer or a few molecular layers within the contact interface between the

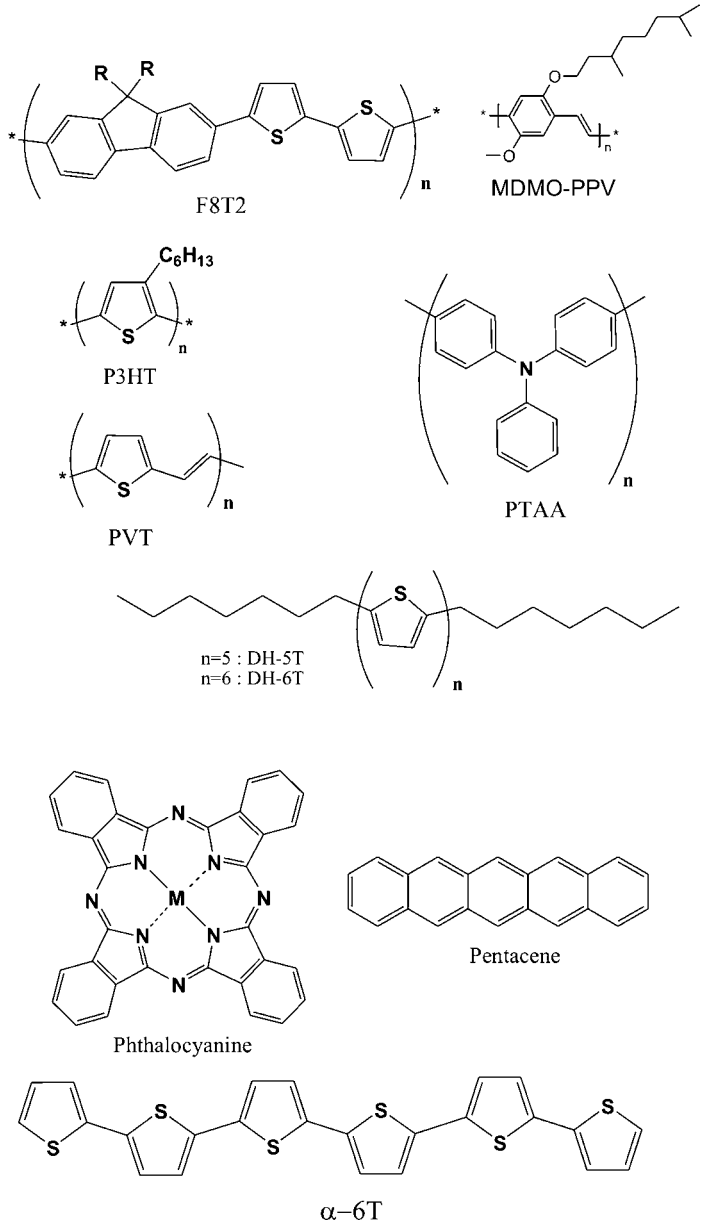

Figure 7 Commonly used *p*-type organic semiconductors. F8T2, poly[9,9′ dioctyl-fluorene-co-bithiophene]; MDMO-PPV, poly[2-methoxy-5-(3,7-dimethyloctyloxy)]-1,4-phenylenevinylene; P3HT, regioregular poly[3-hexylthiophene]; PTAA, polytriarylamine; PVT, poly-[2,5-thienylene vinylene]; DH-5T, α,ω-dihexylquinquethiophene; DH-6T, α,ω-dihexylsexithiophene; phthalocyanine; pentacene; α-6T, α-sexithiophene.

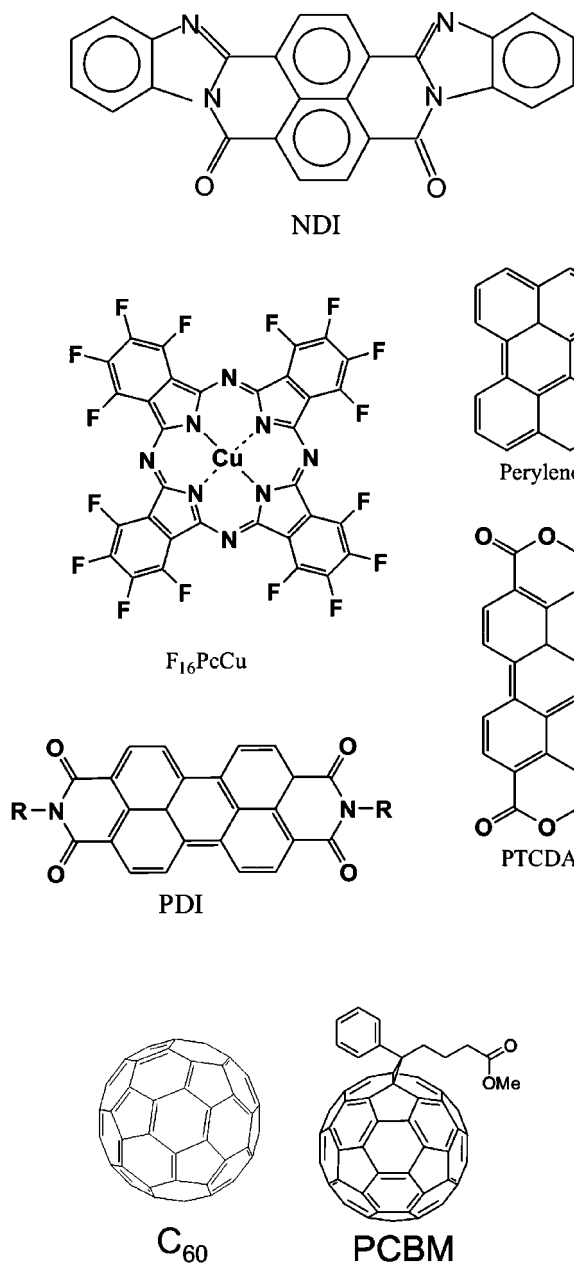

Figure 8 Commonly used *n*-type organic semiconductors. NDI, naphthalene diimide; $F_{16}CuPc$, perfluorocopperphthalocyanine; perylene; PTCDA, 3,4,9,10-perylene-tetracarboxylic dianhydrid and its derivaties; PDI, *N*,*N*′-dimethyl 3,4,9,10-perylene tetracarboxylicdiimide; C_{60}; PCBM, methanofullerene [6,6]-phenyl C_{61}-butyric acid methyl ester.

organic semiconductor and gate dielectric (Figure 9). The first two molecular layers next to the dielectric interface determine the OFET charge transport [Figure 9 (79)]. This is the first direct estimate of the physical thickness of the transport layer in organic TFTs. Hence, the organization of organic semiconductor thin film on the dielectric layer in OFETs is a crucial parameter for device performance (80).

If the interface to the organic dielectric exhibits a large number of chemical groups that can act as charge-carrier traps, this will have a radical influence on charge-carrier transport within the channel. The modification of the interface, on the other hand, can be used to increase and facilitate the charge transport, as shown in Figures 10 and 11 (81).

Most of the pentacene thin films are grown on untreated inorganic SiO_2 or Al_2O_3 dielectrics (82, 83). One of the most significant improvements in the mobility (up to 3.4 $cm^2\ Vs^{-1}$) in pentacene-based OFETs has been achieved by deposition of the pentacene film onto surface-modified Al_2O_3 dielectrics, as shown in Figure 11 (81). The same group demonstrated even higher mobility of 6 $cm^2\ Vs^{-1}$ from pentacene in their later publications (7) in the same year. Surface energy engineering of inorganic/organic dielectric seems to be fine tuning the growth of polycrystalline pentacene film (83, 84).

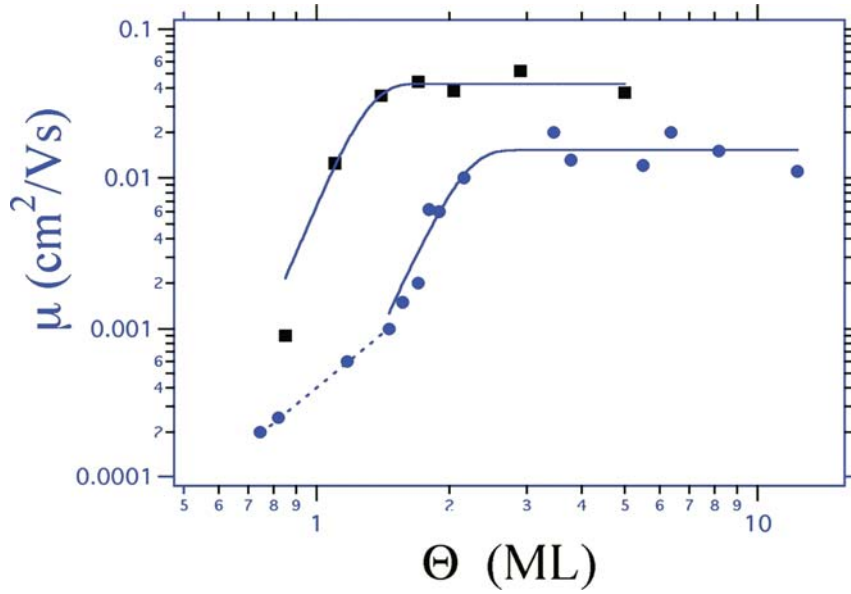

Figure 9 Hole mobility versus coverage (number of monolayers) for low (*squares*) and high (*dots*) rates of deposition. For the high rate series, the mean value of the plateau at room temperature is 1.5 ($\pm$ 0.3) 10^{-2} $cm^2\ Vs^{-1}$. A crossover from monotonic growth to the plateau occurs at $\Theta \approx 2$ ML. Reproduced with permission from Reference 79.

The Nanomorphology of OFETs

The fabrication of OFETs based on C_{60} was reported in 1993; these had a field-effect electron mobility of 10^{-3} cm^2 Vs^{-1} (85). This was followed by a 1995 Bell Laboratories report showing a mobility of 0.3 cm^2 Vs^{-1} (86). This was recently reproduced in OFETs with mobilities of 0.5 cm^2 Vs^{-1} (87). HWE-grown C_{60} on organic dielectrics normally shows mobilities of approximately 0.6 cm^2 Vs^{-1} (88). Recently it was reported that the thin-film morphology of fullerene C_{60} can be influenced heavily by preheating the dielectric substrate at elevated temperatures before deposition (Figure 12) (8). Films grown at higher substrate temperatures yield mobilities of up to 6 cm^2 Vs^{-1}, as shown in Figure 13 (6). Fullerene-based devices are rather sensitive to air, which induces traps and reduces mobility by several orders of magnitude.

Morphological studies of copper phthalocyanine (CuPc) films grown on carbon-coated electron-microscopic grids exhibit nanoscale crystallites, as shown in Figure 14. Correlated with the thin-film morphology, the field-effect mobility is found to be limited by defects, grain size, and grain boundaries varying from 1×10^{-3} cm^2 Vs^{-1} to 3.7×10^{-3} cm^2 Vs^{-1} in these studies (89).

Frisbie and coworkers (90) have studied incidence X-ray diffraction (GIXD) of ultrathin pentacene films thermally evaporated on a SiO_2/Si substrate. From the first few monolayers, in which charge transport dominates, two polymorphs are observed. The monolayer phase has a two-dimensional rectangular cell wherein the long axis of the pentacene molecule is perpendicular to the a-b crystal plane on the dielectric surface. In the thin-film phase, the long axis of the pentacene molecule is slightly tilted with respect to the dielectric surface normal (90). This in turn has important implications for interfacial transport in pentacene-based OFETs.

Sirringhaus and coworkers (91) showed that the performance of polymer OFETs crucially depends on the polymer's chemical and structural ordering. With structural optimization, these microcrystalline polymers can exhibit mobilities beyond 0.1 cm^2 Vs^{-1} (92–94). Thin films of P3HT reveal a highly microcrystalline and anisotropic lamellar microstructure consisting of two-dimensional conjugated layers with strong π–π interchain interactions separated by layers of solubilizing, insulating side chains; this microstructure leads to fast in-plane charge transport (Figure 15) (91). These microcrystals have a nanoribbon shape (93). The field-effect mobility of P3HT is very sensitive to the degree of head-to-tail regioregularity (91, 92) and film-deposition techniques (91, 92). High-molecular-weight P3HT films have varying degrees of crystallinity, which also are induced by varying the solvent (94). The mobility also increases with increasing molecular weight (95), which is attributed to lower grain boundaries limiting the transport in low-molecular-weight samples (90) or, to a less planar polymer backbone in the amorphous regions of the film in the case of low-molecular-weight fractions (96–98).

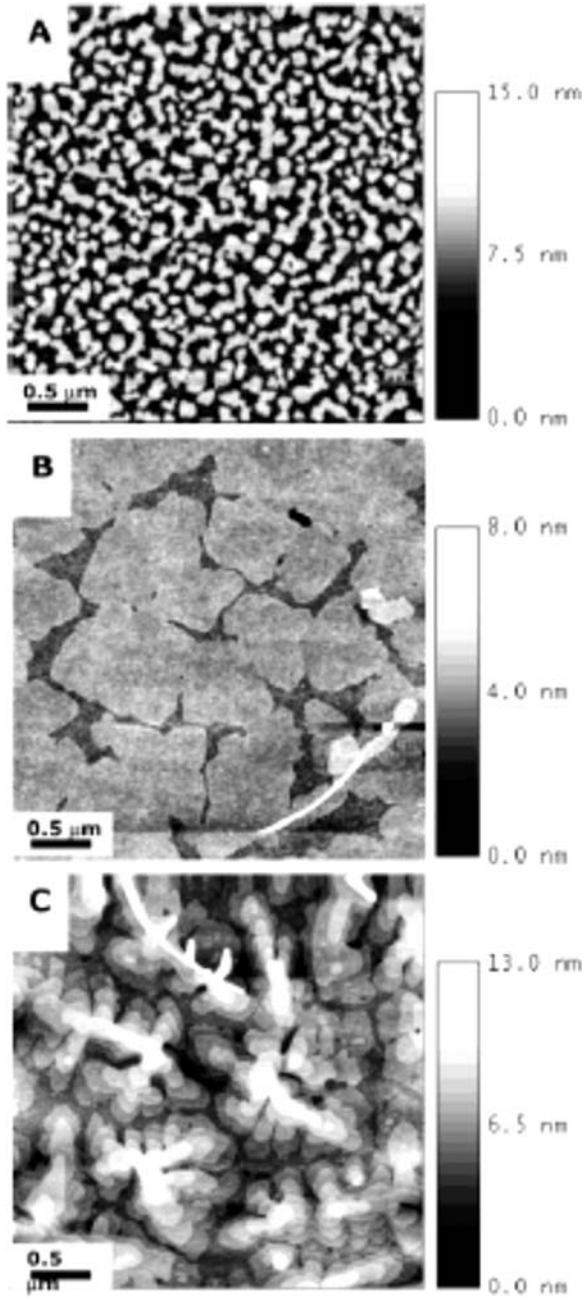

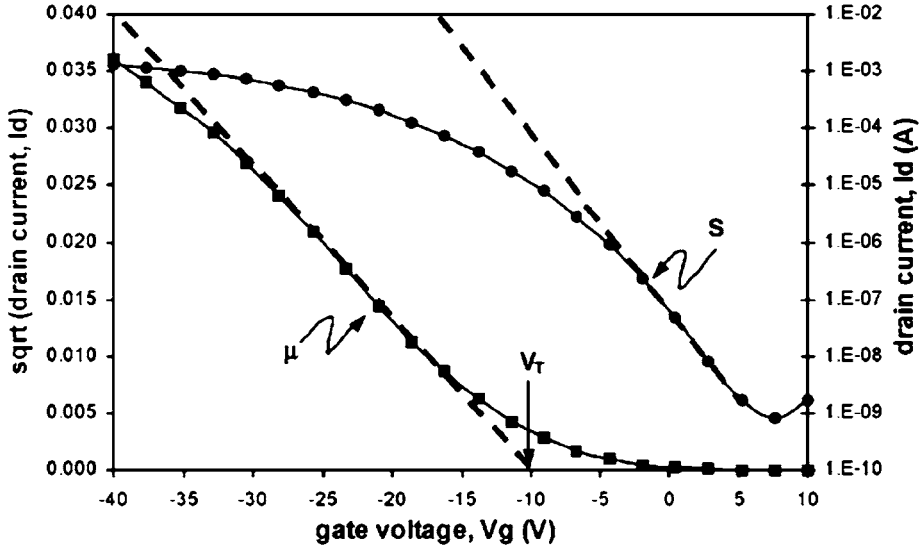

Figure 11 Representative OFET trace for pentacene deposited on an alumina sample treated with 1-phosphonohexadecane. V_{ds} is held constant at -40 V, and V_g is swept from $+10$ to -40 V. A linear fit to the $\sqrt{I_{ds}}$-V_g trace permits the extraction of saturation mobility and threshold voltage (V_T). Device parameters for this sample were $\mu_{sat} = 3.4$ cm^2 Vs^{-1}, $V_T = -10.4$ V, $S = 3.4$ V/decade, and $I_{on}/I_{off} = 1.5 \times 10^6$. Reproduced with permission from Reference 81.

AMBIPOLAR TRANSPORT

The ambipolar charge transport in an organic transistor is a highly desirable property because it enables the design of circuits with lower-power dissipation and good noise margin similar to CMOS logic circuits. It is also a necessary condition for light-emitting transistors (99, 100). Although the first single-channel inorganic

Figure 10 AFM images of 1-phosphonohexadecane with increasing coverage of pentacene. Bright areas in the images are interpreted as increasing film thickness in the *z*, or out-of-plane, direction. (*A*) Initial stages (10-Å coverage) show a large number of nucleation sites and some lateral growth, with no growth in the vertical direction. (*B*) With increasing coverage (35 Å), a second layer of material is nucleated on top of the first layer as the first layer continues to fill in laterally. (*C*) With further pentacene deposition (75 Å), the vertical growth rate seems to more nearly equal to the rate of lateral growth: Several incomplete layers are manifested as lamellae in the pentacene grains. Reproduced with permission from Reference 81.

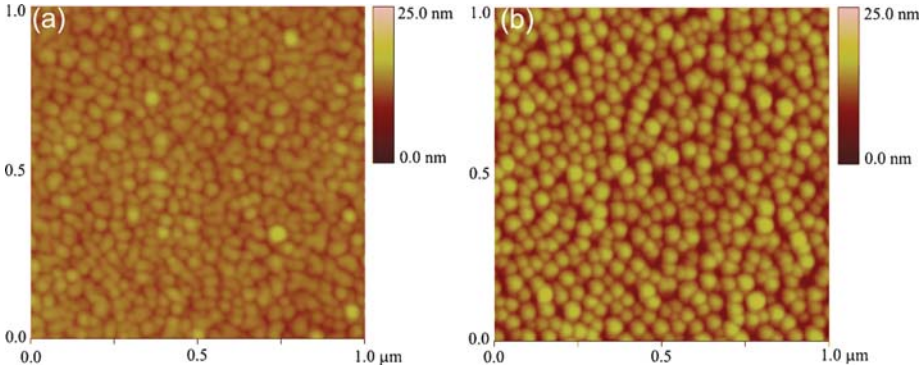

Figure 12 AFM topography images of (a) 5-nm C_{60} film grown on BCB substrates without preheating and (*b*) 5-nm C_{60} film grown on BCB substrates with in-situ preheating at 250°C. Reproduced with permission from Reference 8.

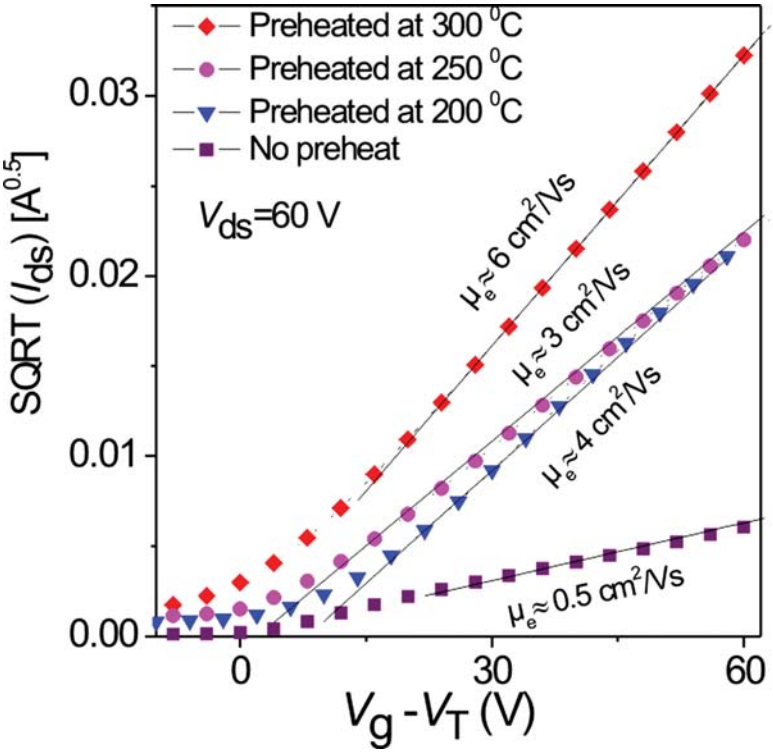

Figure 13 Plots showing $\sqrt{I_{ds}}$ versus V_g-V_T (*symbols*) for C_{60} OFETs fabricated with different growth conditions along with theoretical fit curves (*without symbols*) using Equation 3. The obtained electron mobilities, μ_e, are indicated along with the respective curves. Reproduced with permission from Reference 8.

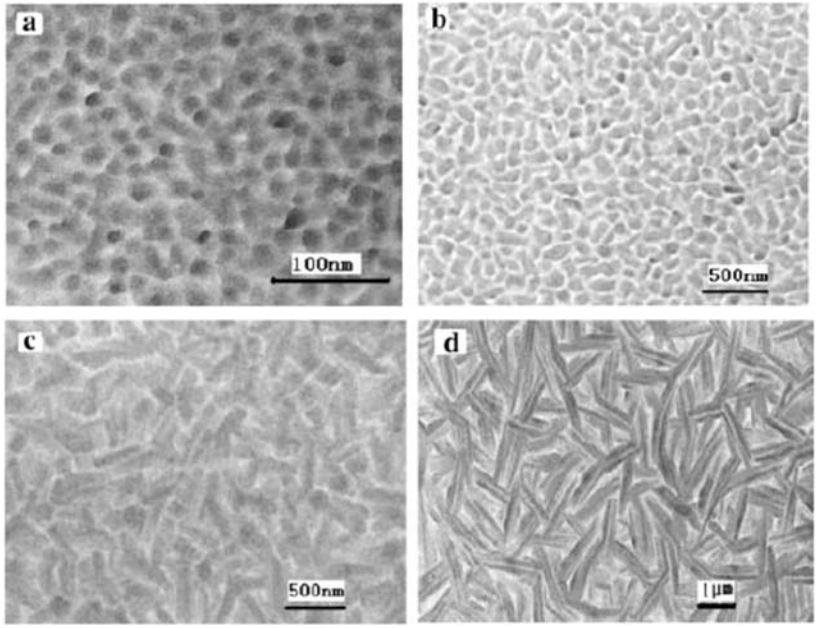

Figure 14 Transmission electron micrographs from CuPc films at different substrate temperatures (T_{sub}). (*a*) At $T_{sub} = 20°C$, crystals are granular and ~20–30 nm in diameter. (*b*) At $T_{sub} = 120°C$, crystals have average dimensions of $\sim 50 \times 200$ nm^2. (*c*) At $T_{sub} = 170°C$, rod-like crystals have average dimensions of $\sim 60 \times 460$ nm^2 (with some small gaps). (*d*) At $T_{sub} = 200°C$, large elongated crystals have dimensions of up to $\sim 400 \times 3000$ nm^2 (with severe discontinuities and large gaps). Reproduced with permission from Reference 89.

ambipolar transistors were demonstrated more than two decades ago (101), they have been reported from organic semiconductors in recent years (102–104). The first report on ambipolar operation in a single OFET was for devices employing a *p*/*n*-type heterostructure as the active channel layer consists of two organic semiconductors (102, 103). It was shown that currents of both polarities could be simultaneously injected from the source and the drain contacts under appropriate bias conditions and that both *n*- and *p*-type transistor operation could be achieved. More recently, ambipolar charge transport was reported for OFETs employing single films of heterogeneous blends consisting of polymer-based interpenetrating networks [first suggested by Tada et al. (103)] as well as for narrow band-gap organic semiconductors (104). Using these materials, the first complementary-like inverters employing single-channel OFETs have been demonstrated (104). In their work, Meijer et al. (104) argued that ambipolar transport is an intrinsic property of pure organic semiconductors and that it is highly dependent on energy-level matching between (*a*) the work function of the source and drain electrodes and

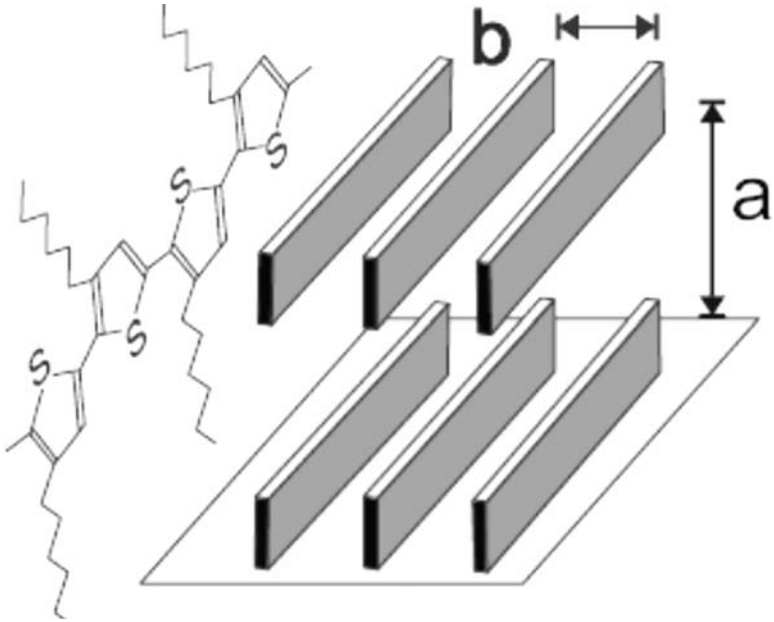

Figure 15 Regioregular poly(3-hexyl thiophene) shows in-plane, lamellar self-organization. *a* and *b* are lattice parameters. Reproduced with permission from Reference 91.

(*b*) the energy levels, namely the highest occupied molecular orbital (HOMO) and lowest unoccupied molecular orbital (LUMO), of the semiconductor (see also Reference 67 and references therein).

Surface energy of a chosen dielectric plays an important role in the orientation and packing of the organic semiconductors on top of it. Charge trapping at the interfacial layer, polarity of the dielectric, and the dielectric polarizability are reported to be responsible for electrical hysteresis (19), bias stress (105), and device degradation (106), for example. Figure 16 shows that the organic semiconductor pentacene can be ambipolar on polyvinylalchohol as dielectrics (57). If the standard Si/SiO_2 dielectric gate transistor geometry is used, normally pentacene will only give *p*-type OFET operation. This demonstrates that using organic dielectrics like PVA can have a fundamental influence on the character of OFETs.

ORGANIC LIGHT-EMITTING TRANSISTORS

We now turn to a discussion of the possible implications of ambipolar transport in OFETs in organic light-emitting transistors (OLETs) (100). The first demonstration of OLETs was performed using a tetracene thin film (102, 107). With the gate

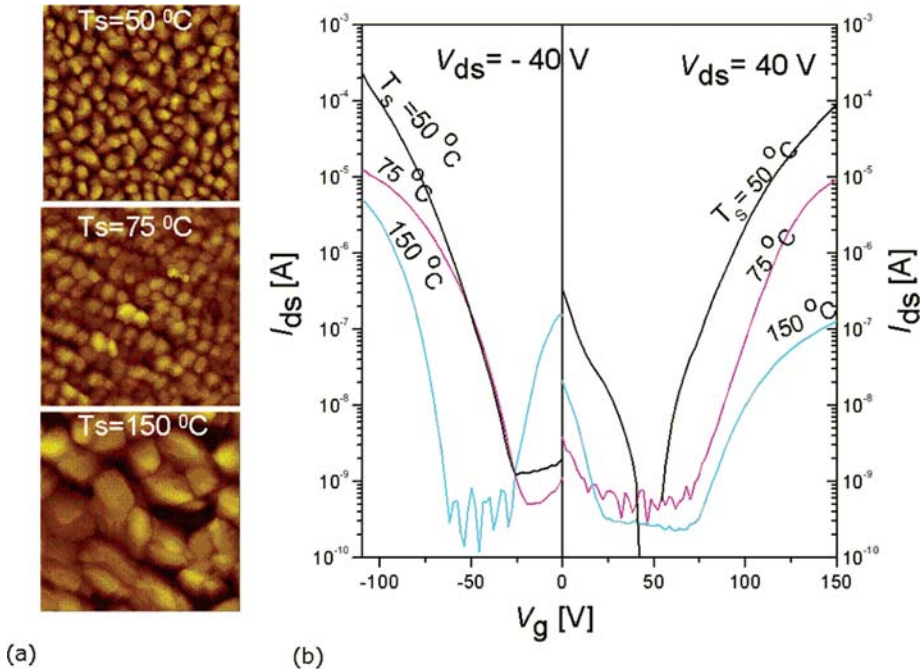

Figure 16 (*a*) AFM images of pentacene film grown on polyvinyl alcohol dielectric at different elevated substrate temperatures. (*b*) Corresponding ambipolar transistor transfer characteristics for both electron-enhanced and hole-enhanced modes.

bias, holes accumulate in the transistor channel. This hole current flows toward the drain, which is negative biased with respect to the source. Together with the direct injection of electrons from the drain into the LUMO level of tetracene, these injected electrons have a high probability of interacting with positively charged tetracene molecules to form excitons, which can then give rise to light emission. However, in unipolar devices, light emission is restricted to a region close to the contact that injects the charge carriers of lower mobility, as shown in Figure 17. In contrast, an ambipolar OLET would allow the electron-hole balance as well as the location of the recombination zone between source and drain to be tuned by the gate voltage, hence improving the quantum efficiency of light emission per injected charge.

Rost et al. (100) have demonstrated OLETs based on coevaporated films of α-pentathiophene (α-5T) and N,N′-ditridecylperylene-3,4,9,10-tetracarbozylic diimide (P13). Balanced charge-carrier mobility seems to be a prerequisite for such devices. Exciton formation and therefore light emission strongly depend on the relative positions of the HOMO and LUMO energy level of the two organic semiconductors.

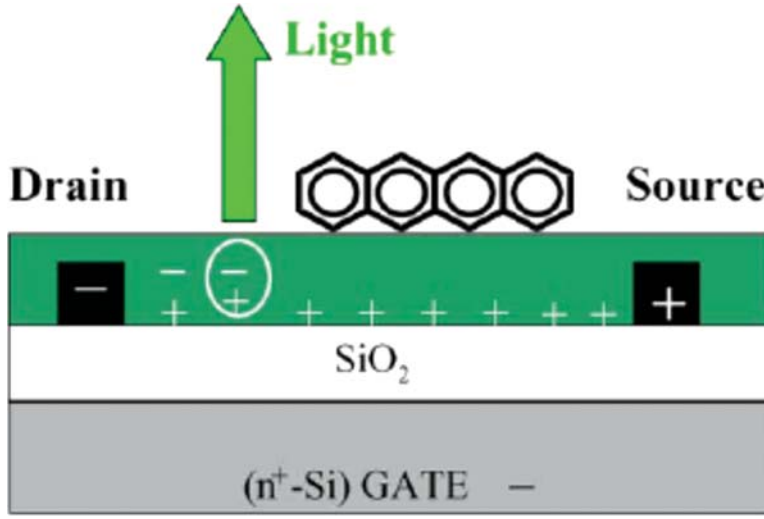

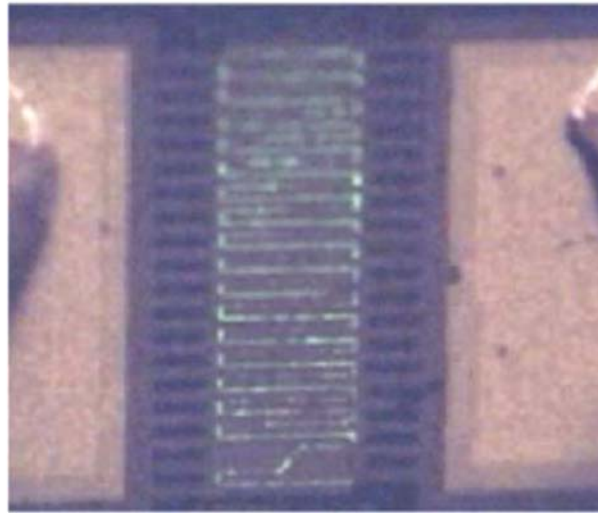

Figure 17 Structure (*top*) and micrographs (*bottom*) of OLETs fabricated on SiO_2/*n*-Si substrates. Light is generated by recombination of holes and electrons injected into the transistor channel by source and drain contacts, respectively. Tetracene as an organic semiconductor and 15-nm sputtered Au as a source-drain electrode were used. Reproduced with permission from Reference 99.

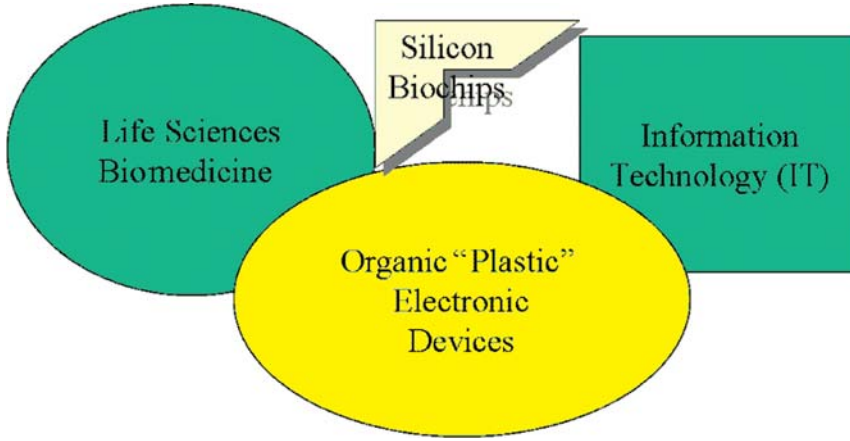

Figure 18 Interfacing the life sciences with electronic technology (cybernetics) may be the future mission of organic semiconductor devices.

CONCLUSIONS

In the field of OFETs, there is a growing interest for use of organic gate insulators in conjunction with organic semiconductors. The low temperature processibility of organic dielectrics fits well with the processing advantages of organic semiconductors. Top-gate geometries became feasible by using organic gate insulators. The large number of organic dielectrics provides enormous practical flexibility.

In this article, we focused on the effects of the interface between organic insulators and organic semiconductors. The first couple of nanometers of organic semiconductors close to the organic dielectric interface play a crucial role in OFET performance. Modification of this interface can change the characteristics of the OFETs considerably. Along with these interfacial effects, the nanomorphology of the organic semiconductors close to the interface also are important for OFET performance. This nanomorphology can be manipulated by varying the temperature, solvent used, or surface modification. With this flexibility and versatility, OFETs using organic dielectrics will be increasingly important for the practical realization of organic integrated circuits.

Furthermore, owing to the compatibility of carbon/hydrogen-based organic semiconductors with organic biomolecules and living cells, there is a great opportunity to integrate such organic semiconductor devices with living organisms. The largely independent fields of bio/life sciences and information technology can be thus bridged in an advanced cybernetic approach, through the use of organic semiconductor devices (Figure 18). Facilitating this interface in the resulting field of bio-organic electronic devices is proposed to be the future mission of organic semiconductor devices.

ACKNOWLEDGMENTS

We acknowledge Dr. Thomas D. Anthopoulos and Dr. Dago M. de Leeuw of Philips Research Laboratories, Eindhoven; Prof. Siegfried Bauer of Soft Matter Physics, JKU Linz; and Prof. Dr. Gilles Horowitz of ITODYS, CNRS-UMR 7086, University Denis-Diderot, Paris and colleagues in LIOS for stimulating discussion and collaboration. We also acknowledge financial support from Austrian Science Foundation, FWF Project Nos. P16891-N08 and N00103000.

LITERATURE CITED

1a. Clemens W, Fix W, Ficker J, Knobloch A, Ullmann A. 2004. From polymer transistors toward printed electronics. *J. Mater. Res.* 19:1963

1b. Horowitz G. 2004. Organic thin film transistors: from theory to real device. *J. Mater. Res.* 19:1946

2. Crone B, Dodabalapur A, Lin Y-Y, Filas RW, Bao Z, et al. 2000. Large-scale complementary integrated circuits based on organic transistors. *Nature* 403:521

3. Huitema HEA, Gelinck GH, van der Putten JBPH, Kuijk KE, Hart CM, et al. 2001. Plastic transistors in active-matrix displays. *Nature* 414:599

4a. Rogers JA, Bao Z, Baldwin K, Dodabalapur A, Crone B, et al. 2001. Paper-like electronic displays: large-area rubber-stamped plastic sheets of electronics and microencapsulated electrophoretic inks. *Proc. Natl. Acad. Sci.USA* 98:4835

4b. Sundar VC, Zaumseil J, Podzorov V, Menard E, Willett RL, et al. 2004. Elastomeric transistor stamps: reversible probing of charge transport in organic crystals. *Science* 303:1644

5. Eder F, Klauk H, Halik M, Zschieschag U, Schmid G, Dehm C. 2004. Organic electronics on paper. *Appl. Phys. Lett*. 84:2673

6. Huitema HE, Gelinck GH, Van Veenendaal E, Cantatore E, Touwslager FJ, et al. 2003. A flexible QVGA display with organic transistors. IDW 1663

7. Kelley TW, Muyres DV, Baude PF, Smith TP, Jones TD. 2003. High performance organic thin film transistors. *Mater. Res. Soc. Symp. Proc.* 771:L6.5.1

8. Singh ThB, Marjanović N, Matt GJ, Günes S, Sariciftci NS, et al. 2005. Enhanced mobility of organic field-effect transistors with epitaxially grown C_{60} film by in-situ heat treatment of the organic dielectric. *Mater. Res. Soc. Symp. Proc*. 871E:I4.9.1

9. Montaigne Ramil A, Singh ThB, Haber NT, Marjanović N, Günes S, et al. 2006. Influence of film growth conditions on carrier mobility of hot wall epitaxially grown fullerene based Transistors. *J. Cryst. Growth*. 288:123

10. Facchetti A, Yoon M-H, Marks TJ. 2005. Gate dielectrics for organic field-effect transistors: new opportunities for organic electronics. *Adv. Mater.* 17:1705

11. Sirringhaus H. 2005. Device physics of dolution-processed organic field-effect transistors. *Adv. Mater.* 17:2411–25

12. Peng X, Horowitz G, Fichou D, Garnier F. 1990. All-organic thin-film transistors made of α-sexithienyl semiconducting and various polymeric insulating layers. *Appl. Phys. Lett.* 57:2013–15

13. Klauk H, Halik M, Zschieschang U, Schmid G, Radlik W. 2002. High-mobility polymer gate dielectric

pentacene thin film transistors. *J. App. Phys.* 92:5259

14. Parashkov R, Becker E, Ginev G, Riedl T, Johannes HH, Kowalsky W. 2004. All-organic thin-film transistors made of poly(3-butylthiophene) semiconducting and various polymeric insulating layers. *J. Appl. Phys.* 95:1594–96
15. Park J, Park SY, Shim S, Kang H, Lee HH. 2004. A polymer gate dielectric for high-mobility polymer thin-film transistors and solvent effects. *Appl. Phys. Lett.* 85:3283–85
16. Schroeder R, Majewski LA, Grell M. 2003. A study of the threshold voltage in pentacene organic field-effect transistors. *Appl. Phys. Lett.* 83:3201–3
17. Knipp D, Street RA, Krusor B, Ho J, Apte RB. 2002. Influence of the dielectric on the growth and performance of pentacene thin-film transistors. *Mat. Res. Soc. Symp. Proc.* 708:BB.10
18. Schroeder R, Majewski LA, Grell M. 2004. All-organic permanent memory transistor using an amorphous, spin-cast ferroelectric-like gate insulator. *Adv. Mater.* 16:633–36
19. Singh ThB, Marjanović N, Matt GJ, Sariciftci NS, Schwödiauer R, Bauer S. 2004. Nonvolatile organic field-effect transistor memory element with a polymeric gate electret. *Appl. Phys. Lett.* 85:5409–11
20. Naber RCG, Tanase C, Blom PWM, Gelinck GH, Marsman AW, et al. 2005. High-performance solution-processed polymer ferroelectric field-effect transistors. *Nat. Mater.* 4:243–48
21. Singh ThB, Marjanović N, Stadler P, Auinger M, Matt GJ, et al. 2005. Fabrication and characterization of solution-processed methanofullerene-based organic field-effect transistors. *J. Appl. Phys.* 97:083714
22. Chua LL, Zaumseil J, Chang J, Ou ECW, Ho PKH, et al. 2005. General observation of *n*-type field-effect behaviour in organic semiconductors. *Nature* 434:194–99
23. Sze SM. 1981. *Physics of Semiconductor Devices*. New York: Wiley-InterScience. 2nd ed.
24. Horowitz G, Hajlaoui R, Bourgouiga R, Hajlaoui M. 1999. Theory of organic field-effect transistors. *Synth. Met.* 101:401
25. Brown AR, Jarrett CP, de Leeuw DM, Matters M. 1997. Field-effect transistors made from solution- processed organic semiconductors. *Synth. Met.* 88:37
26. Horowitz G. 1998. Organic field-effect transistors. *Adv. Mater.* 10:365
27. Sirringhaus H, Brown PJ, Friend RH, Nielsen MM, Bechgaard K, et al. 1999. Two-dimensional charge transport in self-organized, high-mobility conjugated polymers. *Nature* 401:685
28. Sirringhaus H, Wilson RJ, Friend RH, Inbasekaran M, Wu W, et al. 2000. Mobility enhancement in conjugated polymer field-effect transistors through chain alignment in a liquid-crystalline phase. *Appl. Phys. Lett.* 77:406
29. Koezuka H, Tsumara A, Ando T. 1987. Field-effect transistor with polythiophene thin film. *Synth. Met.* 18:699
30. Sirringhaus H, Tessler N, Thomas DS, Brown PJ, Friend RH. 1999. In *Advances in Solid-State Physics*, Vol. 39, ed. B Kramer, pp. 101–10. Wiesbaden, Ger: Vieweg
31. Abdou MSA, Orfino FP, Son Y, Holdcroft S. 1997. Interaction of oxygen with conjugated polymers: charge transfer complex formation with poly(3-alkylthiophenes). *J. Am. Chem. Soc.* 119:4518
32. Ong BS, Wu YL, Liu P, Gardner S. 2004. High-performance semiconducting polythiophenes for organic thin-film transistors. *J. Am. Chem. Soc.* 126:3378
33. Heeney M, Bailey C, Genevicius K, Shkunov M, Sparrow D, et al. 2005. Stable polythiophene semiconductors incorporating thieno[2,3-b]thiophene. *J. Am. Chem. Soc.* 127:1078
34. Deleted in proof
35. Street RA, Salleo A. 2002. Contact effects

in polymer transistors. *Appl. Phys. Lett.* 81:2887

36. van de Craats AM, Stutzmann N, Bunk O, Nielsen MM, Watson M, et al. 2003. Meso-epitaxial solution-growth of self-organizing discotic liquid-crystalline semiconductors. *Adv. Mater.* 15:495
37. Pisula W, Menon A, Stepputat M, Lieberwirth I, Kolb U, et al. 2005. A zone-casting technique for device fabrication of field-effect transistors based on discotic hexa-peri-hexabenzocoronene. *Adv. Mater.* 17:684
38. Herwig PT, Mullen K. 1999. A soluble pentacene precursor: synthesis, solid-state conversion into pentacene and application in a field-effect transistor. *Adv. Mater.* 11:480
39. Afzali A, Dimitrakopoulos CD, Graham TO. 2003. Photosensitive pentacene precursor: synthesis, photothermal patterning, and application in thin-film transistors. *Adv. Mater.* 15:2066
40. Gelinck GH, Geuns TCT, de Leeuw DM. 2000. High-performance all-polymer integrated circuits. *Appl. Phys. Lett.* 77:1487
41. Afzali A, Dimitrakopoulos CD, Breen TL. 2002. High-performance, solution-processed organic thin film transistors from a novel pentacene precursor. *J. Am. Chem. Soc.* 124:8812
42. Aramaki S, Sakai Y, Ono N. 2004. Solution-processible organic semiconductor for transistor applications: tetrabenzoporphyrin. *Appl. Phys. Lett.* 84:2085
43. Chang PC, Lee J, Huang D, Subramanian V, Murphy AR, Frechet JMJ. 2004. Film morphology and thin film transistor performance of solution-processed oligothiophenes. *Chem. Mater.* 16:4783
44. Hotta S, Waragai K. 1991. Alkyl-substituted oligothiophenes: crystallographic and spectroscopic studies of neutral and doped forms. *J. Mater. Chem.* 1:835
45. Garnier F, Yassav A, Hajlaoui R, Horowitz G, Deloffre F, et al. 1993. Molecular engineering of organic semiconductors: design of self-assembly properties in conjugated thiophene oligomers. *J. Am. Chem. Soc.* 115:8716
46. Horowitz G, Fichou D, Peng XZ, Xu ZG, Garnier F. 1989. A field-effect transistor based on conjugated α-sexithienyl. *Solid State Commun.* 72:381
47. Garnier F, Hajlaoui R, Yassar A, Srivastava P. 1994. All polymer field-effect transistor realized by printing techniques. *Science* 265:1684
48. Garnier F. 1996. Thin film transistors based on molecular semiconductors. *Pure Appl. Chem.* 68:1455
49. Katz HE. 1997. Organic molecular solids as thin film transistor semiconductors. *J. Mater. Chem.* 7:369
50. Garnier F, Horowitz G, Peng XZ, Fichou D. 1991. Structural basis for high carrier mobility in conjugated oligomers. *Synth. Met.* 45:163
51. Torsi L, Dodabalapur A, Rothberg LJ, Fung AWP, Katz HE. 1995. Intrinsic transport properties and performance limits of organic field-effect transistors. *Science* 272:1462
52. Katz HE, Torsi L, Dodabalapur A. 1995. Synthesis, material properties, and transistor performance of highly pure thiophene oligomers. *Chem. Mater.* 7:2235
53. Dimitrakopoulos CD, Furman BK, Graham T, Hedge S, Purushothaman S. 1998. Field-effect transistors comprising molecular beam deposited α,ω-di-hexylhexathienylene and polymeric insulator. *Synth. Met.* 92:47
54. Horowitz G, Hajlaoui ME. 2000. Mobility in polycrystalline oligothiophene field-effect transistors dependent on grain size. *Adv. Mater.* 12:1046
55. Halik M, Klauk H, Zschieschang U, Schmid G, Ponomarenko S, et al. 2003. Relationship between molecular structure and electrical performance of oligothiophene organic thin film transistors. *Adv. Mater.* 15:917

56. Gundlack DJ, Lin YY, Jackson TN, Schlom DG. 1997. Oligophenyl-based organic thin film transistors. *Appl. Phys. Lett.* 71:3853
57. Singh ThB, Meghdadi F, Günes S, Marjanović N, Horowitz G, et al. 2005. High-performance ambipolar pentacene organic field-effect transistors on poly(vinylalcohol) organic gate dielectric. *Adv. Mater.* 17:2315
58. Bao Z, Lovinger AJ, Dodabalapur A. 1996. Organic field-effect transistors with high mobility based on copper phthalocyanine. *Appl. Phys. Lett.* 69:3066
59. Bao Z, Lovinger AJ, Dodabalapur A. 1997. Highly ordered vacuum-deposited thin films of metallophthalocyanines and their applications in field-effect transistors. *Adv. Mater.* 9:42
60. Rella R, Serra A, Siciliano P, Tepore A, Zoeco A. 1997. Langmuir-Blodgett multilayers based on copper phthalocyanine as gas sensor materials: active layer-gas interaction model and conductivity modulation. *Langmuir* 13:6562
61. Law KY. 1993. Organic photoconductive materials: recent trends and developments. *Chem. Rev.* 93:449
62. Zhang J, Wang J, Wang H, Yan D. 2004. Organic thin-film transistors in sandwich configuration. *Appl. Phys. Lett.* 84:142
63. Locklin J, Shinbo K, Onishi K, Kaneko F, Bao Z, Advincula C. 2003. Ambipolar organic thin film transistor-like behavior of cationic and anionic phthalocyanines fabricated using layer-by-layer deposition from aqueous solution. *Chem. Mater.* 15:1404
64. Katz HE, Bao Z. 2000. The physical chemistry of organic field-effect transistors. *J. Phys. Chem. B* 104:671
65. Bao Z, Lovinger AJ, Brown J. 1998. New air-stable *n*-channel organic thin film transistors. *J. Am. Chem. Soc.* 120:207
66. Waldauf C, Schilinsky P, Perisutti M, Hauch J, Brabec CJ. 2003. Solution-processed organic *n*-type thin-film transistors. *Adv. Mater.* 15:2084
67. Anthopoulos TD, Tanase C, Setayesh S, Meijer EJ, Hummelen JC, et al. 2004. Ambipolar organic field-effect transistors based on a solution-processed methanofullerene. *Adv. Mater.* 16:2174
68. Chikamatsu M, Nagamatsu S, Yoshida Y, Saito K, Yase K, Kikuchi K. 2005. Solution-processed *n*-type organic thin-film transistors with high field-effect mobility. *Appl. Phys. Lett.* 87:203504
69. Bao Z, Feng Y, Dodabalapur A, Raju VR, Lovinger AJ. 1997. High-performance plastic transistors fabricated by printing techniques. *Chem. Mater.* 9:1299
70. Rogers JA, Bao Z, Makhija A, Braun P. 1999. Printing process suitable for reel-to-reel production of high-performance organic transistors and circuits. *Adv. Mater.* 11:741
71. Xia Y, Whitesides GM. 1998. Soft lithography. *Angew. Chem. Int. Ed.* 37:550
72. Hebner TR, Wu CC, Marcy D, Lu MH, Sturm JC. 1998. Inkjet printing of doped polymers for organic light-emitting devices. *Appl. Phys. Lett.* 72:519
73. Yang Y, Chang SC, Bharathan J, Liu J. 2000. Organic/polymeric electroluminescent devices processed by hybrid inkjet printing. *J. Mater. Sci. Mater. Electron.* 11:89
74. Yokoyama O. 2003. Active-matrix full color organic electroluminescent displays fabricated by ink-jet printing. *Optronics* 254:119
75. Sirringhaus H, Kawase T, Friend RH, Shimoda T, Inbasekaran M, et al. 2000. High-resolution inkjet printing of all-polymer transistor circuits. *Science* 290:2123
76. Blanchet GB, Loo YL, Rogers JA, Gao F, Fincher CR. 2003. Large area, high resolution, dry printing of conducting polymers for organic electronics. *Appl. Phys. Lett.* 82:463
77. Zielke D, Hübler AC, Hahn U, Brandt N, Bartzsch M, et al. 2005. Polymer-based organic field-effect transistor using offset printed source/drain structures. *Appl. Phys. Lett.* 87:123508

78. Andreev A, Matt G, Brabec CJ, Sitter H, Badt D, et al. 2000. Highly anisotropically self-assembled structures of parasexiphenyl grown by hot wall epitaxy. *Adv. Mater.* 12:629
79. Dinelli F, Murgia M, Levy P, Cavallini M, Biscarini F, de Leeuw DM. 2004. Spatially correlated charge transport in organic thin film transistors. *Phys. Rev. Lett.* 92:116802
80. Loi MA, Como ED, Dinelli F, Murgia M, Zamboni R, et al. 2005. Supramolecular organization in ultra-thin films of α-sexithiophene on silicon dioxide. *Nat. Mater.* 4:81
81. Kelly TW, Boardman LD, Dunbar TD, Muyres DV, Pellerite MJ, Smith TP. 2003. High-performance OTFTs using surface-modified alumina dielectrics. *J. Phys. Chem. B* 107:5877
82. Lin Y-Y, Gundlach DJ, Nelson SF, Jackson TN. 1997. Stacked pentacene layer organic thin-film transistors with improved characteristics. *IEEE Electron. Devices Lett.* 18:606
83. Nelson SF, Lin Y-Y, Gundlach DJ, Jackson TN. 1998. Temperature-independent transport in high-mobility pentacene transistors. *Appl. Phys. Lett.* 72:1854
84. Yang SY, Shin K, Park CE. 2005. Effect of gate-dielectric surface energy on the pentacene morphology and the organic field-effect transistor characteristics. *Adv. Mater.* 15:1806
85. Kastner J, Paloheimo J, Kuzmany H. 1993. Fullerene field effect transistor. In *Electronic Properties of High-T_c Superconductors*, *Springer Series in Solid State Sciences, Vol. 113*, ed. H Kuzmany, M Mehring, J Fink, pp. 512–15. Berlin: Springer-Verlag
86. Haddon RC, Perel AS, Morris RC, Palstra TTM, Hebard AF. 1995. C_{60} thin film transistors. *Appl. Phys. Lett.* 67: 121
87. Kobayashi S, Takenobu T, Mori S, Fujiwara A, Iwasa Y. 2003. Fabrication and characterization of C_{60} thin-film transistors with high field-effect mobility. *Appl. Phys. Lett.* 82:4581
88. Singh ThB, Marjanović N, Matt GJ, Gunes S, Sariciftci NS, et al. 2005. High-mobility *n*-channel organic field-effect transistors based on epitaxially grown C_{60} films. *Organic Electronics* 6:105
89. Xiao K, Liu Y, Yu G, Zhu D. 2003. Influence of the substrate temperature during deposition on film characteristics of copper phthalocyanine and field-effect transistor properties. *Appl. Phys. A* 77:367
90. Fritz SE, Martin SM, Frisbie CD, Ward MD, Toney MF. 2004. Structural characterization of a pentacene monolayer on an amorphous SiO_2 substrate with grazing incidence X-ray diffraction. *J. Am. Chem. Soc.* 126:4084
91. Sirringhaus H, Tessler N, Friend RH. 1998. Integrated optoelectronic devices based on conjugated polymers. *Science* 280:1741
92. Bao Z, Dodabalapur A, Lovinger AJ. 1996. Soluble and processable regioregular poly(3-hexylthiophene) for thin film field-effect transistor applications with high mobility. *Appl. Phys. Lett.* 69:4108
93. Bjornholm T, Hassenkam T, Greve DR, McCullough RD, Jayaraman M, et al. 1999. Polythiophene nanowires. *Adv. Mater.* 11:1218
94. Chang JF, Sun BQ, Breiby DW, Nielsen MM, Solling TI, et al. 2004. Enhanced mobility of poly(3-hexylthiophene) transistors by spin-coating from high-boiling-point solvents. *Chem. Mater.* 16:4772
95. Kline RJ, McGehee MD, Kadnikova EN, Liu JS, Frechet JMJ. 2003. Controlling the field-effect mobility of regioregular polythiophene by changing the molecular weight. *Adv. Mater.* 15:1519
96. Zhao N, Botton GA, Zhu SP, Duft A, Ong BS, et al. 2004. Microscopic studies on liquid crystal poly(3,3‴-dialkylquaterthiophene) semiconductor. *Macromolecules* 37:8307
97. Wang GM, Swensen J, Moses D, Heeger AJ. 2003. Increased mobility from

regioregular poly(3-hexylthiophene) field-effect transistors. *J. Appl. Phys.* 93:6137

98. Zen A, Pflaum J, Hirschmann S, Zhuang W, Jaiser F, et al. 2004. Effect of molecular weight and annealing of poly(3-hexylthiophene)s on the performance of organic field-effect transistors. *Adv. Funct. Mater.* 14:757
99. Santato C, Capelli R, Loi MA, Murgia M, Cicoira F, et al. 2004. Tetracene-based organic light-emitting transistors: optoelectronic properties and electron injection mechanism. *Synthetic Metals* 146:329
100. Rost C, Karg S, Reiss W, Loi MA, Murgia M, Muccini M. 2004. Ambipolar light-emitting organic field-effect transistor. *Appl. Phys. Lett.* 85:1613
101. Matsumura M, Nara Y. 1980. High-performance amorphous-silicon field-effect transistors. *J. Appl. Phys.* 51: 6443
102. Dodabalapur A, Katz HE, Torsi L, Haddon RC. 1996. Organic field-effect bipolar transistors. *Appl. Phys. Lett.* 68:1108
103. Tada K, Harada H, Yoshino K. 1996. Polymeric bipolar thin-film transistor utilizing conducting polymer containing electron transport dye. *Jpn. J. Appl. Phys.* 35:L944
104. Meijer EJ, de Leeuw DM, Setayesh S, Van Veenendaal E, Huisman B-H, et al. 2003. Solution-processed ambipolar organic field-effect transistors and inverters. *Nat. Mater.* 2:678
105. Sallelo A, Chabinyc ML, Yang MS, Street RA. 2002. Polymer thin-film transistors with chemically modified dielectric interfaces. *Appl. Phys. Lett.* 81:4383
106. Ficker J, von Seggern H, Rost H, Fix W, Clemens W, McCulloch I. 2004. Influence of intensive light exposure on polymer field-effect transistors. A*ppl. Phys. Lett.* 85:1377
107. Hepp A, Heil H, Weise W, Ahles M, Schmechel R, Von Seggern H. 2003. Light-emitting field-effect transistor based on a tetracene thin film. *Phys. Rev. Lett.* 91:157406
108. Ebisawa F, Kurokawa T, Nara S. 1983. Electrical properties of polyacetylene/polysiloxane interface. *J. Appl. Phys.* 54:3255
109. Tsumura A, Koezuka H, Ando T. 1986. Macromolecular electronic device: field-effect transistor with a polythiophene thin film. *Appl. Phys. Lett.* 49:1210
110. Burroughes JH, Jones CA, Friend RH. 1988. New semiconductor device physics in polymer diodes and transistors. *Nature* 335:137
111. Clarisse C, Riou MT, Gauneau M, Le Contellec M. 1988. Field-effect transistor with diphthalocyanine thin film. *Electron. Lett.* 24:674
112. Assadi A, Svensson C, Willander M, Inganäs O. 1988. Field-effect mobility of poly(3-hexylthiophene). *Appl. Phys. Lett.* 53:195
113. Paloheimo J, Punkka E, Stubb H, Kuivalainen P. 1989. *Lower Dimensional Systems and Molecular Devices*, *Proceedings of NATO ASI*, Spetses, Greece, New York: Plenum Press
114. Horowitz G, Peng X, Fichou D, Garnier F. 1992. Role of semiconductor/insulator interface in the characteristics of *p*-conjugated-oligomer-based thin-film transistors. *Synth. Met.* 51:419
115. Dimitrakopoulos CD, Brown AR, Pomp A. 1996. Molecular beam deposited thin films of pentacene for organic field effect transistor applications. *J. Appl. Phys.* 80:2501
116. Lin Y-Y, Gundlach DJ, Jackson TN. 1996. *High mobility pentacene organic thin film transistors*. Presented at Annu. Device Res. Conf. Digest, Santa Barbara, CA
117. Sirringhaus H, Friend RH, Li XC, Moratti SC, Holmes AB, N. Feeder. 1997. Bis(dithienothiophene) organic field effect transistors with high ON/OFF ratio. *Appl. Phys. Lett.* 71:3871
118. Katz HE, Lovinger AJ, Laquindanum JG. 1998. a–v-dihexylquaterthiophene: a second thin film single-crystal organic semiconductor. *Chem. Mater.* 10:457

119. Laquindanum JG, Katz HE, Lovinger AJ. 1998. Synthesis, morphology, and field-effect mobility of anthradithiophenes. *J. Amer. Chem. Soc.* 120:664
120. Katz HE, Lovinger AJ, Johnson J, Kloc C, Siergist T, et al. 2000. A soluble and air-stable organic semiconductor with high electron mobility. *Nature* 404:478
121. Halik M, Klauk H, Zschieschang U, Kriem T, Schmid G, et al. 2002. Fully patterned all-organic thin film transistors. *Appl. Phys. Lett.* 81:289
122. Malenfant PRL, Dimitrakopoulos CD, Gelorme JD, Kosbar LL, Graham TO. 2002. *n*-type organic thin-film transistor with high field-effect mobility based on a *N,N*-dialkyl-3,4,9,10-perylene tetracarboxylic diimide derivative. *Appl. Phys. Lett.* 80:2517
123. Chesterfield RJ, Newman CR, Pappenfus TM, Ewbank PC, Haukaas MH, et al. 2003. High electron mobility and ambipolar transport in organic thin-film transistors based on π-stacking quinoidal terthiophene. *Adv. Mater*. 15:1278
124. Hadamani BH, Natelson D. 2004. Temperature-dependent contact resistances in high-quality polymer field-effect transistors. *Appl. Phys. Lett.* 84:443
125. Chesterfield RJ, McKeen JC, Newman ChR, Frisbie CD, Ewbank PC, et al. 2004. Variable temperature film and contact resistance measurements on operating *n*-channel organic thin film transistors. *J. Appl. Phys.* 95:6396
126. Masayuki C, Nagamatsu S, Taima T, Yoshida Y, Sakai N, et al. 2005. C_{60} thin-film transistors with low work-function metal electrodes. *Appl. Phys. Lett.* 85:2396
127. Wang G, Hirasa T, Moses D, Heeger AJ. 2004. Fabrication of regioregular poly(3-hexylthiophene) field-effect transistors by dip-coating. *Synth. Met.* 146:127
128. Wu Y, Liu P, Gardner S, Ong BS. 2005. Poly(3,3″-dialkylterthiophene)s: room-temperature, solution-processed, high-mobility semiconductors for organic thin-film transistors. *Chem. Mater.* 17:221
129. Majewski LA, Schroeder R, Voigt M, Grell M. 2004. High performance organic transistors on cheap, commercial substrates. *J. Phys. D* 37:3367

Annual Review of Materials Research
Volume 36, 2006

CONTENTS

POROUS AND COLLOIDAL MATERIALS

CURRENT INTEREST